

Report: Synthesis of optimal filter for MHOQ

July 9, 2024

Contents

1	Quantisation	2
2	Noise shaping quantiser	2
3	Moving horizon optimal quantiser (MHOQ)	2
3.1	Alternative binary formulation	3
4	Noise Transfer Function(NTF)	3
5	Spectrum of quantisation noise	4
6	Synthesis of optimal noise-shaping filter	6
6.1	Optimal noise shaping filter with constraint	6
6.1.1	System	7
6.1.2	Constraint 1	7
6.1.3	Constraint 2	7
6.1.4	Optimization problem: State Space formulation	7
6.2	LMI Synthesis: Convert BMIs to convex LMIs	8
6.3	Optimization Problem:	9
7	Simulation: Optimal noise shaping	10
7.1	Simulation 1:	10
8	Switching Frequency Minimization	13
9	MPC with switching rate limitation:	15
10	Closed Form Solution:	16
10.1	Prediction horizon $N = 1$:	16
10.2	Prediction horizon $N = 2$:	17
11	Scribble	18

1 Quantisation

Let $w \in \mathbb{R}$ be the input, \mathbf{Q} be the quantiser and $y \in \mathbb{U}$ the quantiser output, as shown in the additive model of quantisation in the Figure 1. Let us define the quantisation error as

$$q = \mathbf{Q}(w) - w = y - w. \quad (1)$$

The quantisation requires the signal to be mapped to a finite signal where each value of the output y is restricted to

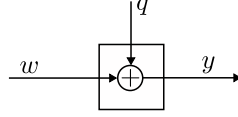


Figure 1: Quantiser additive model

belong to a finite set \mathbb{U} . The elements of the set \mathbb{U} represent the quantiser levels and depends on the word-size of the quantiser.

2 Noise shaping quantiser

Noise-shaping quantisers can reduce the effective quantisation error by moving quantisation noise to higher frequencies through oversampling and feedback. The reconstruction filter is then used to attenuate the frequency-shaped quantisation noise. It operates by estimating the uniform quantisation error and employing a feedback filter to shape the noise power at the output of the DAC. A block diagram for a noise-shaping quantiser is shown in Fig. 3. The feedback filter $F(z)$ is designed such that the transfer function $y = (1 - F(z))\epsilon$ is a high-pass filter.

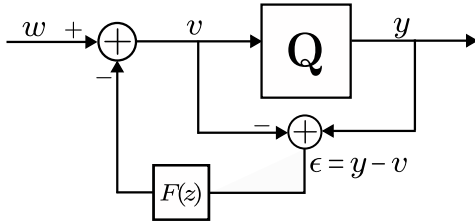


Figure 2: Noise shaping quantiser

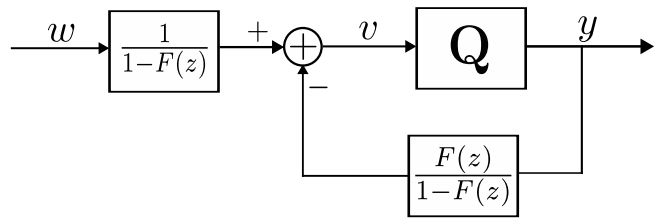


Figure 3: Noise shaping quantiser

In linear analysis, the output is given by

$$Y(z) = \mathbf{STF}.W(z) + \mathbf{NTF}.E(Z) \quad (2)$$

where the signal transfer function $\mathbf{STF} = 1$, noise transfer function $\mathbf{NTF} = (1 - F)$ with F being a noise shaping filter. $F = z^{-1}$ is the special case known as the first-order delta-sigma modulator.

3 Moving horizon optimal quantiser (MHOQ)

The design criteria for the MHOQ is the minimization of the perceived errors defined as follows:

$$e(t) = H(z)(w(t) - y(t)) \quad (3)$$

where $H(z)$ is a stable time-invariant linear low-pass filter with the following state-space

$$H(z) = 1 + C(zI - A)^{-1}B \quad (4)$$

The error e then can be written as the output of the following state-space representation of H

$$\begin{aligned} x(t+1) &= Ax(t) + B(w(t) - y(t)) \\ e(t) &= Cx(t) + w(t) - y(t) \end{aligned} \quad (5)$$

where $x \in \mathbb{R}^n$ is the state vector. The error e corresponds to the difference between the filtered quantised signal and the filtered input signal.

For moving horizon implementation, the optimisation problem is defined as the problem of finding $y \in \mathbb{U}$ that minimises the cost function while satisfying the state equations as follows:

$$y^*(t) = \arg \min_{y(t)} V_N = \sum_{t=k}^{k+N-1} e^2(t) \quad (6)$$

subject to

$$x(t+1) = Ax(t) + B(w(t) - y(t)) \quad (7)$$

$$e(t) = Cx(t) + w(t) - y(t) \quad (8)$$

$$y(t) \in \mathbb{U}. \quad (9)$$

3.1 Alternative binary formulation

The optimization problem (6)-(9) can be reformulated as an optimization problem with the binary variables. Let \mathcal{B} be the number of bits. $b_i = \{0, 1\}$ and $Q_i, i = \{0, 1, \dots, 2^{\mathcal{B}} - 1\}$, be the binary variables and quantisation levels, respectively.

$$y^*(t) = \arg \min_{y(t)} V_N = \sum_{t=k}^{k+N-1} e^2(t) \quad (10)$$

subject to

$$x(t+1) = Ax(t) + B(w(t) - y(t)) \quad (11)$$

$$e(t) = Cx(t) + (w(t) - y(t)) \quad (12)$$

$$y(t) = \sum_{i=0}^{2^{\mathcal{B}}-1} Q_i b_i, \quad \sum_{i=0}^{2^{\mathcal{B}}-1} b_i = 1, \quad b_i = \{0, 1\}. \quad (13)$$

4 Noise Transfer Function(NTF)

The frequency response of the noise transfer functions due to butterworth filters at different cutoff frequencies are shown in the figure Fig. 4. In the figure, we can see that the net area under the curve remain the same. In Fig. 5 the frequency reponse of the low pass filter is plotted along with that of the noise transefer function. This observation shows that the better performance can be achieved by increasing the cutoff frequency during MHOQ while keeping the cutoff frequency of the reconstruction as same. The simulation results in the following table confirm this observation.

Table 1: ENOB at different cutoff frequencies. Reconstruction filter: Butterworth LPF with $n = 2$, $F_c = 100\text{kHz}$ and $F_s = 1\text{Mhz}$.

Fc	100 kHz	200 kHz	300 kHz	400 kHz	500 kHz
ENOB	3.981	5.307	7.817	10.481	10.936

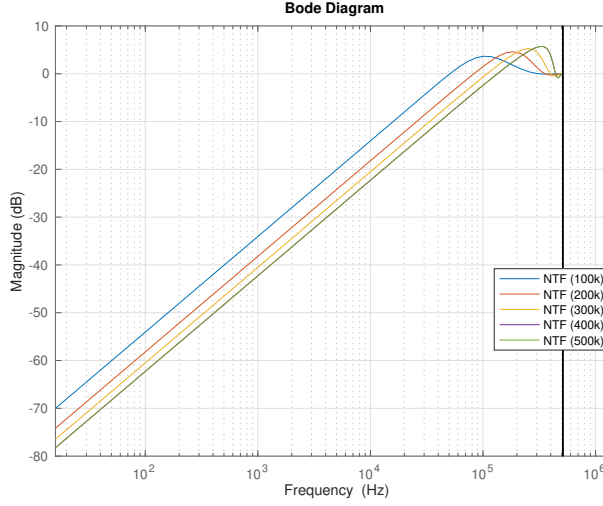


Figure 4: Frequency response of NTF for different cutoff frequency

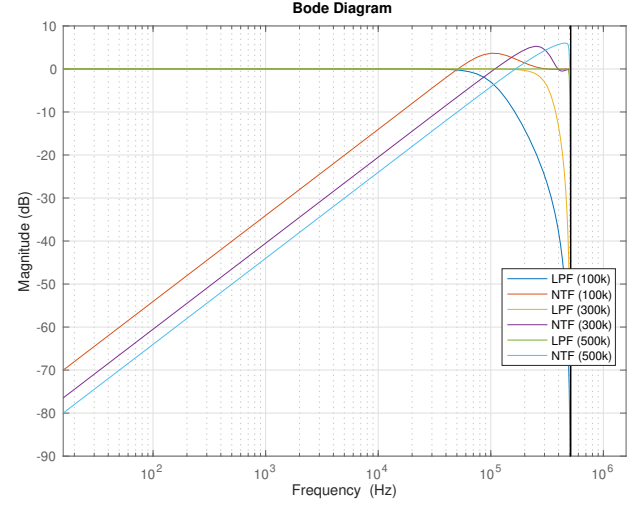


Figure 5: Frequency response of LPF and NTF for different cutoff frequency

5 Spectrum of quantisation noise

The sampling frequency effects the spectrum of the quantisation noise and consequently the ENOB as shown in the following figures.

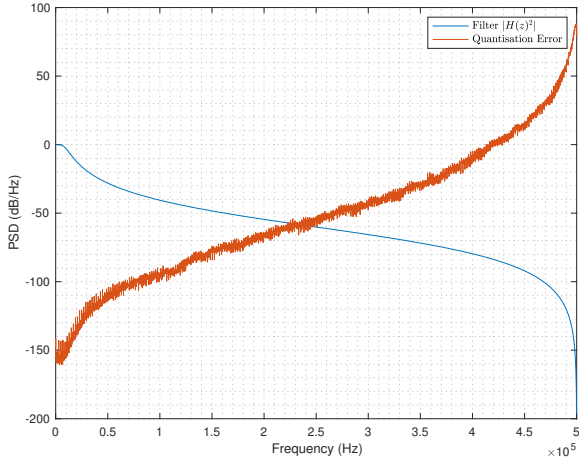


Figure 6: Butterworth Frequency response and frequency spectrum of quantisation noise:
 $F_c = 10 \text{ kHz}$, $F_s = 1 \text{ MHz}$, $ENOB = 16.58$, INL

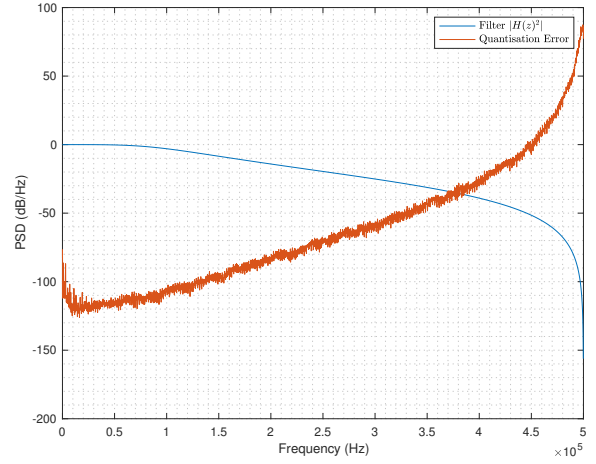


Figure 7: Butterworth Frequency response and frequency spectrum of quantisation noise:
 $F_c = 100 \text{ kHz}$, $F_s = 1 \text{ MHz}$, $ENOB = 7.43$, INL

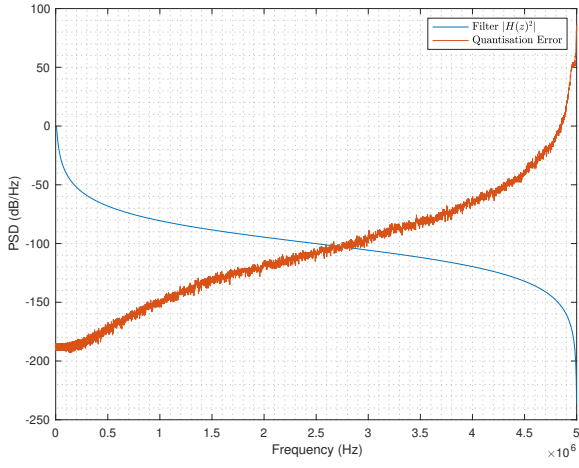


Figure 8: Butterworth Frequency response and frequency spectrum of quantisation noise:
F_c = 10 kHz, F_s = 10 MHz, ENOB = 25.12, INL

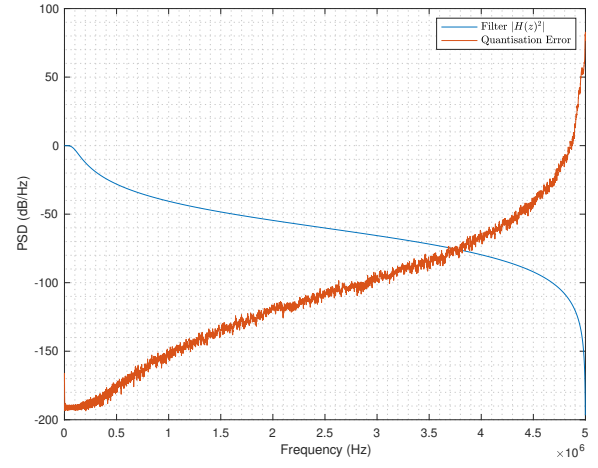


Figure 9: Butterworth Frequency response and frequency spectrum of quantisation noise:
F_c = 100 kHz, F_s = 10 MHz, ENOB = 17.03, INL

6 Synthesis of optimal noise-shaping filter

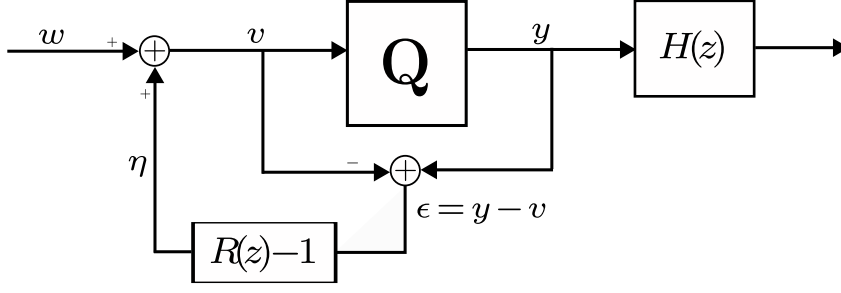


Figure 10: Noise shaping quantiser and a filter $H(z)$.

In noise shaping quantiser with error-feedback structure as shown in the Figure 10, the input to the quantiser is $v = w + \eta = w + (R(z) - 1)\epsilon$ and feedback error ϵ is

$$\epsilon = y - v = y - w - (R(z) - 1)\epsilon. \quad (14)$$

Then quantisation noise defined as $q := y - w$ can be expressed as

$$q = y - w = R(z)\epsilon. \quad (15)$$

Then the effect of the quantisation error on the system $H(z)$ can be expressed as

$$e = H(z)R(z)\epsilon. \quad (16)$$

and it shows that we can reduce the error in the plant output by properly designing the noise shaping filter $R(z)$ with the knowledge of the plant $H(z)$.

The objective is to design stable noise-shaping filter such that it minimises the effect of the quantisation noise in the plant output. A constraint on the error feedback signal should be imposed to prevent the quantiser from overloading and achieve a stable noise-shaping quantiser as

$$\eta = (R(z) - 1)\epsilon.$$

- **Design Problem:** For a fixed pair (p, q) [1],

$$\begin{aligned} & \min_{R(z) \in \mathbb{RH}_\infty} \|e\|_p \\ & \text{subject to.} \\ & R(\infty) = 1, \\ & \|\eta\|_q < \gamma_\eta \end{aligned} \quad (17)$$

where $\mathbb{RH}_\infty = \mathbb{R} \cap \mathbb{H}_\infty$ is the set of proper stable rational transfer functions.

6.1 Optimal noise shaping filter with constraint

The optimization problem is setup as the minimization of the upper bound of the $\|e\|_p$ and $\|\eta_q\|$ as follows:

$$\min_{R(z) \in \mathbb{RH}_\infty} \gamma_e \quad (18)$$

subject to $R(\infty) = 1$ and

$$\|H(z)R(z)\|_{ind.p} < \gamma_e \quad (19)$$

$$\|R(z) - 1\|_{ind.q} < \gamma_\eta \quad (20)$$

where $\|\cdot\|_{ind.r}$ is the induced norm and γ_e and γ_η are the upper bound of $\|H(z)R(z)\|_{ind.p}$ and $\|R(z) - 1\|_{ind.q}$, respectively.

State space representation

6.1.1 System

Denoting the state-space representation of the $H(z)$ and $R(z)$ as (A_h, B_h, C_h, D_h) and $(A_r, B_r, C_r, 1)$ respectively, the state space realization of $H(z)R(z)$ is

$$x_{k+1} = Ax_k + B\epsilon_k \quad (21)$$

$$e_k = Cx_k + D\epsilon_k \quad (22)$$

where

$$A = \begin{bmatrix} A_h & B_h C_r \\ \mathbf{0} & A_r \end{bmatrix} \quad B = \begin{bmatrix} B_h \\ B_r \end{bmatrix} \quad C = [C_h \quad D_h C_r] \quad D = D_h. \quad (23)$$

Similary, the variance of the error e under the white noise assumption at time k in state-space form is given by \mathbb{H}_2 -norm as

$$\|H(z)R(z)\|_2^2 = \sum_{k=0}^{\infty} \|CA^k B\|_2^2 + DD^\top. \quad (24)$$

Moreover, if A is Schur matrix, then there exists a positive semi-definite solution P of the discrete Lyapunov equation defined as

$$P = A^\top P A + BB^\top \quad (25)$$

and the squared \mathbb{H}_2 norm is given by

$$\|H(z)R(z)\|_2^2 = CPC^\top + DD^\top. \quad (26)$$

6.1.2 Constraint 1

Then $\|H(z)R(z)\|_2 < \gamma_e$ if and only if there exist a positive definite matrix P such that

$$\text{(BMI)} \quad \begin{bmatrix} P & PA & PB \\ A^\top & P & \mathbf{0} \\ B^\top & \mathbf{0} & 1 \end{bmatrix} \succ 0 \quad (27)$$

$$\text{(LMI)} \quad \begin{bmatrix} \mu_e & C & D \\ C^\top & P & \mathbf{0} \\ D^\top & \mathbf{0} & 1 \end{bmatrix} \succ 0 \quad (28)$$

$$\mu_e = \gamma_e^2. \quad (29)$$

6.1.3 Constraint 2

The variance of the noise shaping filter is given by

$$E\{|\eta_k|^2\} = \|R(z) - 1\|_2^2 = \sum_{k=1}^{\infty} \|\tilde{C}A^k B\|_2^2, \quad (30)$$

where $\tilde{C} = [\mathbf{0} \quad C_r]$. Then $\|R(z) - 1\|_2 < \gamma_\eta$ if and only if there exist a positive definite matrix P that satisfies

$$\text{(BMI)} \quad \begin{bmatrix} P & PA & PB \\ A^\top & P & \mathbf{0} \\ B^\top & \mathbf{0} & 1 \end{bmatrix} \succ 0 \quad (31)$$

$$\text{(LMI)} \quad \begin{bmatrix} \mu_\eta & \tilde{C} \\ \tilde{C}^\top & P \end{bmatrix} \succ 0 \quad (32)$$

$$\mu_\eta = \gamma_\eta^2. \quad (33)$$

6.1.4 Optimization problem: State Space formulation

Thus the optimization problem can be written as follows,

$$\min_{R(z) \in \mathbb{RH}_\infty} \gamma_e \quad (34)$$

subject to $R(\infty) = 1$ and

$$\begin{bmatrix} P & PA & PB \\ A^\top & P & \mathbf{0} \\ B^\top & \mathbf{0} & 1 \end{bmatrix} \succ 0 \quad (35)$$

$$\begin{bmatrix} \mu_e & C & D \\ C^\top & P & \mathbf{0} \\ D^\top & \mathbf{0} & 1 \end{bmatrix} \succ 0 \quad (36)$$

$$\begin{bmatrix} \mu_\eta & \tilde{C} \\ \tilde{C}^\top & P \end{bmatrix} \succ 0 \quad (37)$$

$$\mu_e = \gamma_e^2, \mu_\eta = \gamma_\eta^2. \quad (38)$$

6.2 LMI Synthesis: Convert BMIs to convex LMIs

BMIs are not convex and NP hard to solve, but they can be converted to convex LMIs and can be solved numerically whereas the LMIs are convex. The non-convex BMIs can be converted to convex LMIs using change of variables [2].

Change of Variables:

Let the order of $H(z)$ is n and the set of $n \times n$ positive define matrices is denoted as $\text{PD}(n)$. Denote by \mathcal{P} the set of variables $\mathbf{p} = \{P_f, P_g, W_f, W_g, W_h, L\}$ where $P_f \in \text{PD}(n)$, $P_g \in \text{PD}(n)$, $W_f \in \mathbb{R}^{1 \times n}$, $W_g \in \mathbb{R}^{n \times 1}$, $W_h \in \mathbb{R}$ and $L \in \mathbb{R}^{n \times n}$. Then define the following matrix values function on \mathcal{P} :

$$\begin{aligned} M_A &:= \begin{bmatrix} A_h P_f + B_h W_f & A_h \\ L & P_g A_h \end{bmatrix} \\ M_B &:= \begin{bmatrix} B_h \\ W_g \end{bmatrix} \\ M_C &:= [C_h P_f + D_h W_f \quad C_h] \\ M_P &:= \begin{bmatrix} P_f & I_n \\ I_n & P_g \end{bmatrix}. \end{aligned} \quad (39)$$

Next, define

$$P^{-1} := \begin{bmatrix} P_f & S_f \\ S_f^\top & P_g \end{bmatrix}, \quad U := \begin{bmatrix} P_f & I_n \\ S_f & \mathbf{0} \end{bmatrix} \quad \text{and} \quad (40)$$

$$S_f := P_f - P_g^{-1}(\succ 0) \quad (41)$$

then we have,

$$M_P = U^\top P U. \quad (42)$$

If the matrices (A_r, B_r, C_r) are given by

$$\begin{aligned} A_r &:= [B_h W_f - P_g^{-1}(L - P_g A_h P_f)] S_f^{-1} \\ B_r &:= [B_h - P_g^{-1} W_g] \\ C_r &:= W_f S_f^{-1} \end{aligned} \quad (43)$$

then (A, B, C) satisfy,

$$M_A = U^\top P A U \quad (44)$$

$$M_B = U^\top P B \quad (45)$$

$$M_C = C U \quad (46)$$

$$M_p = U^\top P U. \quad (47)$$

Multiplying with the transformation $\phi = \text{diag}(U, U, 1)$ form the RHS and ϕ^\top from the LHS the BMI condition 35 takes the following form:

$$\begin{bmatrix} M_P & M_A & M_B \\ M_A^\top & M_P & \mathbf{0} \\ M_B^\top & \mathbf{0} & \mathbf{I} \end{bmatrix} \succ 0. \quad (48)$$

Similarly, using the transformation $\text{diag}(1, U, 1)$, the LMI condition 36 is

$$\begin{bmatrix} \mu_e & M_C & D^\top \\ M_C^\top & M_P & \mathbf{0} \\ D & \mathbf{0} & \mathbf{I} \end{bmatrix} \succ 0 \quad (49)$$

and finally the constraint 37 using the transformation is

$$\begin{bmatrix} \gamma_\eta^2 & M_{\tilde{C}} \\ M_{\tilde{C}}^\top & M_P \end{bmatrix} \succ 0 \quad (50)$$

with $M_{\tilde{C}} := \tilde{C}U$. The LMI conditions 48, 49 and 50 are convex and the minimization of γ_e with these constraints is a convex optimization problem.

6.3 Optimization Problem:

With the change of the variables the BMI is converted to the LMI and since all the LMIs are convex, the optimization problem is a convex optimization problem. Also, since the objective is linear and the constraints are LMIs and with linearity constraints, the optimization problem is Semi-Definite Program (SDP). Such SDP can be solved numerically using CVX. The optimization problem takes the following form,

$$\min \mu_e = \gamma_e^2 \quad (51)$$

subject to,

$$\begin{bmatrix} M_P & M_A & M_B \\ M_A^\top & M_P & \mathbf{0} \\ M_B^\top & \mathbf{0} & \mathbf{I} \end{bmatrix} \succ 0 \quad (52)$$

$$\begin{bmatrix} \mu_e & M_C & D^\top \\ M_C^\top & M_P & \mathbf{0} \\ D & \mathbf{0} & \mathbf{I} \end{bmatrix} \succ 0. \quad (53)$$

$$\begin{bmatrix} \mu_\eta & M_{\tilde{C}} \\ M_{\tilde{C}}^\top & M_P \end{bmatrix} \succ 0 \quad (54)$$

where μ_e is the variance of the output error and μ_η the variance of the feedback error.

7 Simulation: Optimal noise shaping

Notations:

Let us denote the transfer function of a Butterworth low pass filter as $H(z)$. Then from Figure 10, the noise transfer function (NTF) is denoted by $R(z)$ and comparing Figure 2 and Figure 10, the noise shaping transfer function $F(z) = 1 - R(z)$. Moreover, it is shown in the moving horizon implementation of the quantisation [3], the low-pass filter and the noise shaping filter are related as follows,

$$F(z) = \frac{H(z) - 1}{H(z)} \quad \Leftrightarrow \quad H(z) = \frac{1}{1 - F(z)} = \frac{1}{R(z)}. \quad (55)$$

Next, let the optimal noise transfer function (NTF) for low-pass filter $H(z)$ obtained by solving the optimization problem (51)-(54) is denoted as $R_{opt}(z) = \frac{b_r}{a_r}$, where b_r and a_r are the numerator and denominator of the noise transfer function, respectively. Then the optimal noise-shaping transfer function (NSF) is $F_{opt}(z) = 1 - R_{opt}(z) = \frac{a_r - b_r}{a_r}$. Finally, the optimal low pass filter for MPC implementation is $H_{mpc} = \frac{1}{R_{opt}(z)} = \frac{a_r}{b_r}$.

7.1 Simulation 1:

Let us consider a third-order butter-worth low pass filter $H(z)$ with $F_c = 100kHz$ and $F_s = 1Mhz$. Then, from the expression in the equation 55 the corresponding noise shaping filter $F(z)$ and the noise transfer function $R(z)$ can be obtained. Next, the optimization problem (51)-(54) with the constraint $\gamma_\eta < 1.5^2$ (Lee's condition) is solved to obtain the optimal noise transfer function $R_{opt}(z)$ and consequently the $F_{opt}(z)$ and $H_{mpc}(z)$ are obtained. The frequency responses of $H(z)$, $F(z)$ and $R(z)$ are shown in the Figure. 11 and that of $H_{opt}(z)$, $F_{opt}(z)$ and $R_{opt}(z)$ are shown in Figure 12.

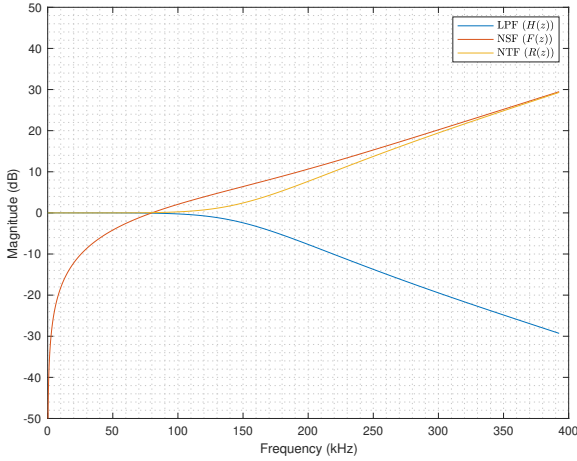


Figure 11: Frequency response: Butterworth filter $H(z)$ with $n = 3$ and $F_c = 100kHz$ and corresponding noise shaping filter $F(z)$ and noise transfer function $R(z)$.

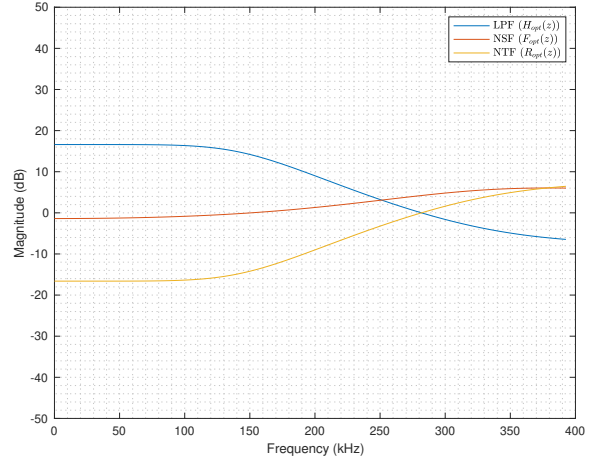


Figure 12: Frequency response: Optimal noise transfer function $R_{opt}(z)$ for $H(z)$ and corresponding noise shaping filter $F_{opt}(z)$ and low pass filter $H_{opt}(z)$.

Table 2: ENOB obtained for different methods with uniform quantisation models. Optimal NTF solved for second order butterworth filter with $F_c = 100kHz$ and $F_s = 1Mhz$.

ENOB/ Methods	Direct	DSM	NSD (Optimal)	MPC ($N = 1$)	MPC ($N = 2$)	MPC ($N = 3$)
6-bit	6.936	8.291	9.30	9.30	9.303	9.361
8-bit	9.650	10.366	11.357	11.357	11.326	11.380
12-bit	13.285	14.365	15.372	15.372	15.290	15.281
16-bit	17.148	18.390	19.373	19.373	19.247	19.134

Table 3: ENOB obtained for different methods with nonlinear quantisation models. Optimal NTF solved for second order butterworth filter with $F_c = 100kHz$ and $F_s = 1Mhz$.

ENOB/ Methods	Direct	DSM	NSD (Optimal)	MPC ($N = 1$)	MPC ($N = 2$)	MPC ($N = 3$)
6-bit	4.177	7.977	7.022	7.022	6.99	7.007
8-bit	6.526	9.968	9.228	9.228	9.251	9.241
12-bit	10.830	13.679	13.524	13.524	13.503	13.509
16-bit	13.577	15.77	16.156	16.156	16.157	16.145

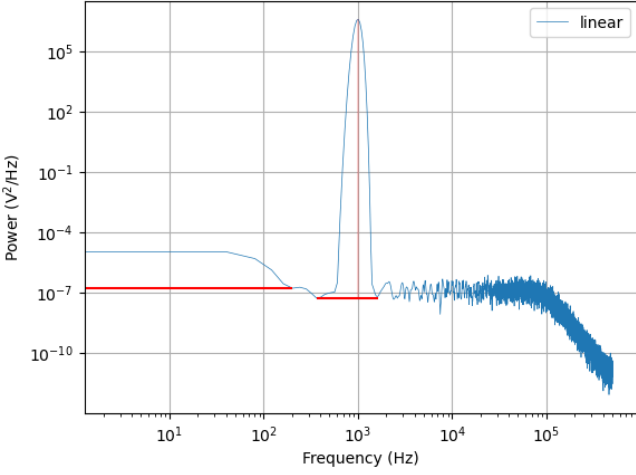


Figure 13: Direct Quantisation

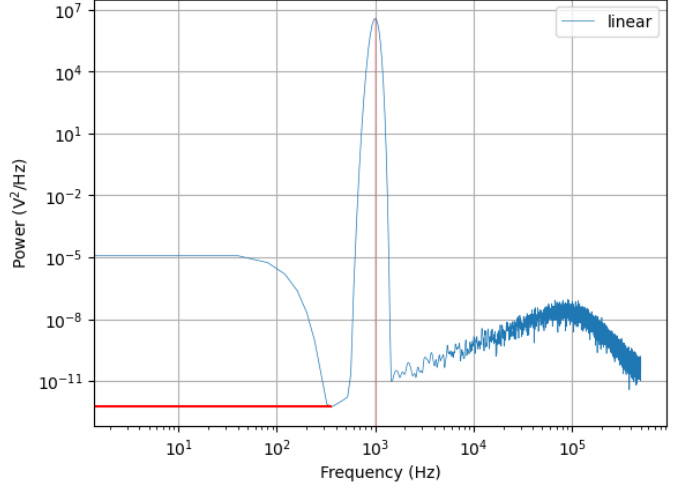


Figure 14: Delta sigma modulator

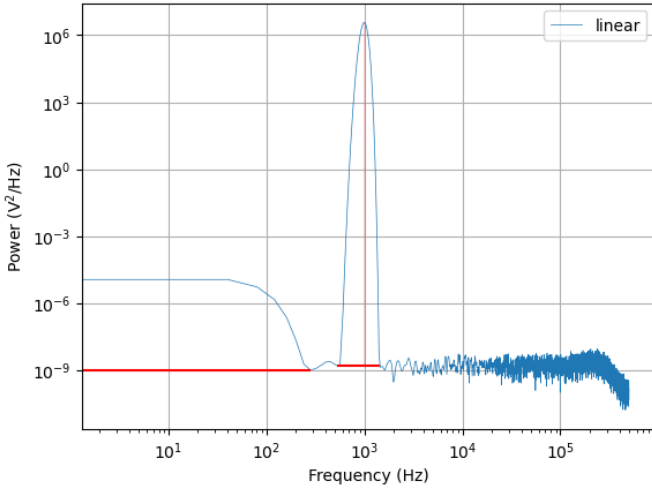


Figure 15: Noise shaping quantiser

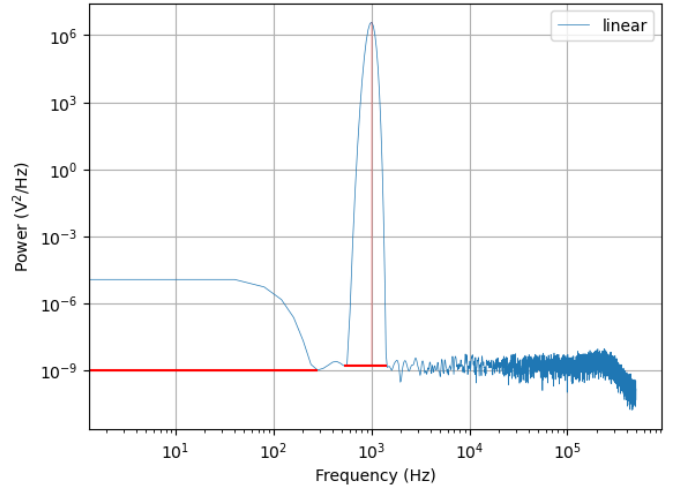


Figure 16: MPC with optimal noise shaping

Table 4: ENOB obtained for different methods with nonlinear quantisation models. Optimal NTF solved for second order butterworth filter with $F_c = 100kHz$ and $F_s = 10Mhz$.

ENOB/ Methods	Direct	DSM	NSD (Optimal)	MPC ($N = 1$)	MPC ($N = 2$)	MPC ($N = 3$)
6-bit	5.041	12.355	15.576	15.576	15.548	15.577
8-bit	7.392	13.950	16.988	16.988	16.406	17.008
12-bit	11.210	17.368	20.952	20.952	20.950	20.931
16-bit	13.877	19.413	23.369	23.369	23.372	23.372

Table 5: ENOB for different values of γ_η

Methods/ γ_η	1.5	2	3	4	5	6	7	8	9	10	11	12
Direct	17.148	-	-	-	-	-	-	-	-	-	-	-
DSM	18.390	-	-	-	-	-	-	-	-	-	-	-
NSD	19.152	19.370	19.532	19.522	19.472	19.339	19.222	19.127	18.976	18.705	2.786	2.2.458
MPC(N=1)	19.152	19.370	19.532	19.522	19.472	19.339	19.222	19.127	18.976	18.705	2.786	2.458
MPC(N=2)	19.098	19.237	19.533	19.402	19.301	19.191	19.023	18.909	18.787	18.738	18.641	18.577
MPC(N=3)	18.955	19.133	19.266	19.180	19.040	18.868	18.746	18.677	18.638	18.560	18.456	18.379

Table 6: ENOB for different values of γ_η using 16 bit DAC.

γ_η / Headroom	0	10	20	30	40	50	60	70	80	90
1.5	19.152	19.066	19.004	18.924	18.830	18.728	18.616	18.531	18.412	18.278
3	19.532	19.455	19.387	19.313	19.210	19.117	19.028	18.904	18.793	18.676
9	18.976	18.980	18.983	18.826	18.747	18.640	18.527	18.429	18.314	18.187
10	18.705	18.877	18.807	18.728	18.637	18.549	18.439	18.340	18.225	18.090
11	2.786	18.814	18.719	18.622	18.546	18.457	18.341	18.245	18.129	18.00
12	2.458	18.700	18.634	18.543	18.447	18.340	18.269	18.142	18.032	17.911
15	1.898	18.457	18.366	18.285	18.192	18.102	18.101	17.897	17.790	17.665
20	1.647	18.118								
30	1.398	17.602								
100	1.398	15.964								
1000	0.828	12.642	12.545	12.484						
10000	0.826	0.631	0.495	10.318	10.25	10.187	10.139	9.925	9.847	9.788

Table 7: ENOB obtained for different methods with nonlinear quantisation models. Optimal NTF solved for second order butterworth filter with $F_c = 100kHz$ and $F_s = 1Mhz$.

ENOB/ Methods	Direct	DSM	NSD (Optimal)	MPC ($N = 1$) [Time (s)]	MPC ($N = 2$) [Time (s)]	MPC ($N = 3$)
6-bit (BINARY)	6.693	8.322	9.051	9.051 [≈ 880 s]	9.135 [≈ 3820 s]	-
6-bit (SCALED)	6.693	8.322	9.051	9.051 [≈ 120 s]	9.093 [≈ 380 s]	9.141 [≈ 450 s]

8 Switching Frequency Minimization

The optimization problem (6)-(9) can be reformulated as an optimization problem with the binary variables. Let \mathcal{B} be the number of bits. $b_i = \{0, 1\}$ and $Q_i, i = \{0, 1, \dots, 2^{\mathcal{B}} - 1\}$, be the binary variables and quantisation levels, respectively.

$$y^*(t) = \arg \min_{y(t)} V_N = \sum_{t=k}^{k+N-1} e^2(t) + \beta \mathcal{N}_s \quad (56)$$

subject to

$$x(t+1) = Ax(t) + B(w(t) - y(t)) \quad (57)$$

$$e(t) = Cx(t) + (w(t) - y(t)) \quad (58)$$

$$y(t) = \sum_{i=0}^{2^{\mathcal{B}}-1} Q_i b_i(t), \quad \sum_{i=0}^{2^{\mathcal{B}}-1} b_i(t) = 1, \quad b_i = \{0, 1\}. \quad (59)$$

$$\mathcal{N}_s = \sum_{i=0}^{2^{\mathcal{B}}-1} |b_i(t) - b_i(t-1)|^2 \quad (60)$$

where $b_i(t-1)$ is the state of the switch i at the previous state and $b_i(t)$ is the state of switch i at the current state and β is the weighting factor.

Table 8: Simulation Results: Carrier Frequency 999Hz, Total number of samples: 21021.

Weighting Factor (β)	0	0.1	0.5	1	5	10	100
ENOB	9.392	9.374	8.694	8.036	6.574	6.080	4.000
Total number of switches (% switching of total number of samples)	16238 ($\approx 77\%$)	15213 ($\approx 72\%$)	13875 ($\approx 66\%$)	13233 ($\approx 63\%$)	11582 ($\approx 55\%$)	10912 ($\approx 52\%$)	9376 ($\approx 45\%$)

Table 9: Simulation Results: Carrier Frequency 99Hz, Total number of samples: 111111.

Weighting Factor (β)	0	0.1	0.5	1	5	10	100
ENOB	9.444	9.177	8.693	8.158	6.833	5.845	3.733
Total number of switches (% switching of total number of samples)	85548 ($\approx 77\%$)	79474 ($\approx 72\%$)	70175 ($\approx 63\%$)	68803 ($\approx 62\%$)	53833($\approx 48\%$)	53319($\approx 48\%$)	43703 ($\approx 39\%$)

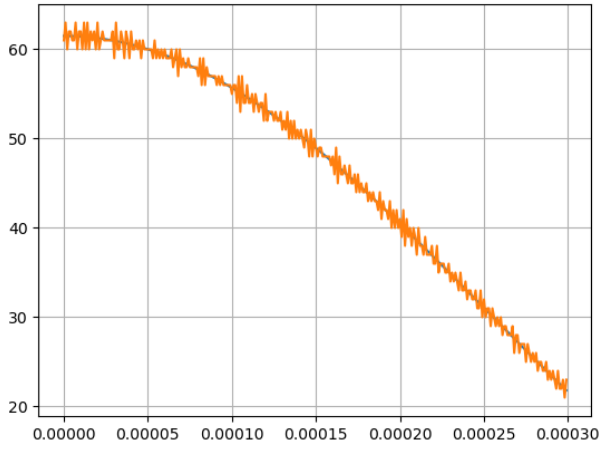


Figure 17: Carrier frequency: $999Hz, \beta = 0$

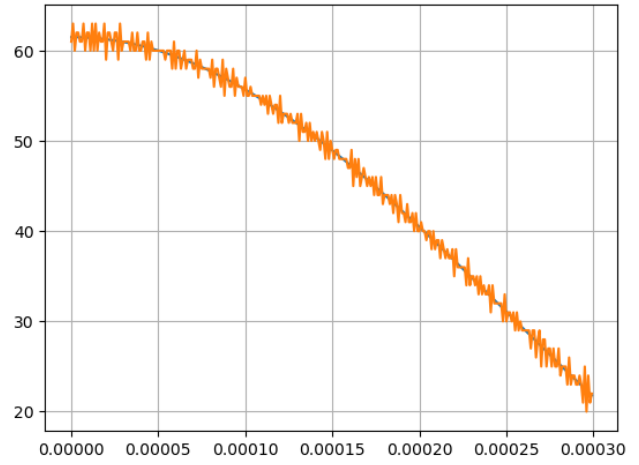


Figure 18: Carrier frequency: $999Hz, \beta = 0.1$

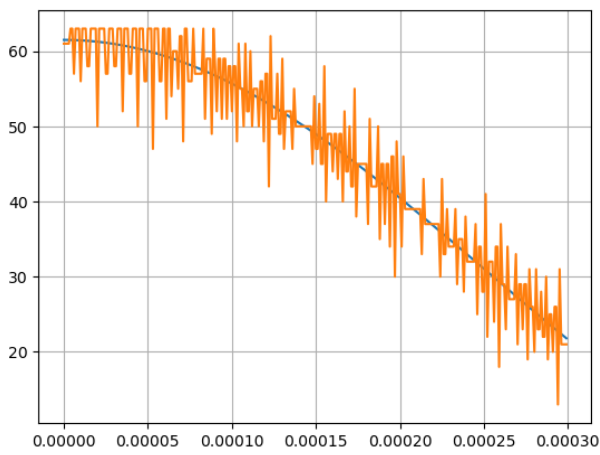


Figure 19: Carrier frequency: $999Hz, \beta = 10$

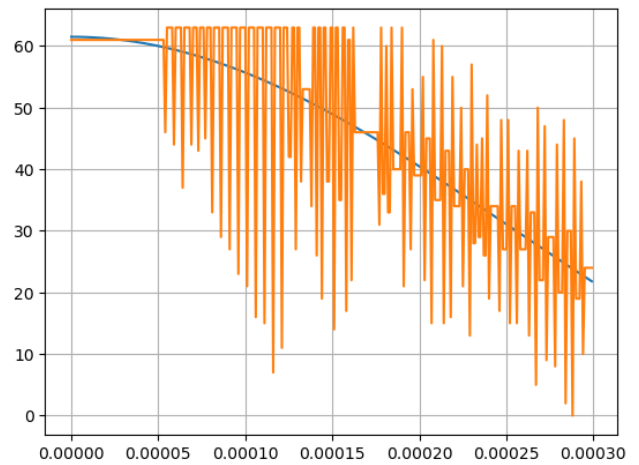


Figure 20: Carrier frequency: $999Hz, \beta = 100$

9 MPC with switching rate limitation:

The MPC formulation with the rate limitation is as follows:

$$y^*(t) = \arg \min_{y(t)} V_N = \sum_{t=k}^{k+N-1} e^2(t) \quad (61)$$

subject to

$$x(t+1) = Ax(t) + B(w(t) - y(t)) \quad (62)$$

$$e(t) = Cx(t) + w(t) - y(t) \quad (63)$$

$$y(t) \in \mathbb{U}. \quad (64)$$

10 Closed Form Solution:

Let N be the prediction horizon of the moving horizon implementation and \mathbb{U} the quantisation levels. The N th power cartesian product of the set \mathbb{U} for N is defined as $\mathbb{U}^N := \mathbb{U} \times \dots \times \mathbb{U}$. Let $n_{\mathbb{U}}$ represent the number of element in the set \mathbb{U} i.e., number of quantisation levels, then the number of elements on the set \mathbb{U}^N is $n_{\mathbb{U}}^N$. Also, let $v_i, i = \{1, 2, \dots, n_{\mathbb{U}}^N\}$ represent the elements of the set \mathbb{U}^N . Then, the closed form solution of the moving horizon implementation of the optimisation problem (6)-(9) is

$$\mathbf{y}^*(k) = \Psi^{-1} q_{\tilde{\mathbb{U}}^N} [\Psi \mathbf{w}(k) + \Gamma x(k)] \quad (65)$$

where

$$\mathbf{y}^*(k) = \begin{bmatrix} y(k) \\ y(k+1) \\ \vdots \\ y(k+N-1) \end{bmatrix}, \quad \mathbf{w}(k) = \begin{bmatrix} w(k) \\ w(k+1) \\ \vdots \\ w(k+N-1) \end{bmatrix}, \quad \Gamma = \begin{bmatrix} C \\ CA \\ \vdots \\ CA^{N-1} \end{bmatrix}, \quad \Psi = \begin{bmatrix} h_0 & 0 & \dots & 0 \\ h_1 & h_0 & \ddots & \vdots \\ \vdots & \ddots & \ddots & 0 \\ h_{N-1} & \dots & h_1 & h_0 \end{bmatrix},$$

and $q_{\tilde{\mathbb{U}}^N}[\cdot]$ represent the nearest neighbor vector quantisation (direct quantisation) and image of this mapping is the set

$$\tilde{\mathbb{U}}^N := \{\tilde{v}_1, \tilde{v}_2, \dots, \tilde{v}_r\} \subset \mathbb{R}^N, \quad r = n_{\tilde{\mathbb{U}}}^N,$$

with $\tilde{v}_i = \Psi v_i$ and $v_i \in \mathbb{U}^N = \{v_1, v_2, \dots, v_{n_{\mathbb{U}}^N}\}$. The elements of the matrices Ψ , $\{h_0, h_1, \dots, h_{N-1}\}$ are the impulse response of the filter $H(z) = 1 + C(zI - A)^{-1}B$ and $h_0 = 1$.

The moving horizon implementation of the above solution is

$$y(k) = [1, 0, \dots, 0] \mathbf{y}^*(k) = [1, 0, \dots, 0] \Psi^{-1} q_{\tilde{\mathbb{U}}^N} [\Psi \mathbf{w}(k) + \Gamma x(k)]. \quad (66)$$

Replacing $x(k) = (zI - A)^{-1}B(a(k) - u(k))$ and with further manipulation, we get,

$$y(k) = [1, 0, \dots, 0] \Psi^{-1} q_{\tilde{\mathbb{U}}^N} [\Psi \{ \mathcal{H}(z) \mathbf{w}(k) - [\mathcal{H}(z) - I] \mathbf{y}^*(k) \}]. \quad (67)$$

where

$$\mathcal{H}(z) = \begin{bmatrix} 1 + \mathcal{H}'_1(z) & 0 & \dots & \dots & 0 \\ \mathcal{H}'_2(z) & 1 & 0 & \dots & 0 \\ \mathcal{H}'_3(z) & 0 & 1 & \dots & 0 \\ \vdots & \vdots & \ddots & \ddots & \vdots \\ \mathcal{H}'_N(z) & 0 & 0 & \dots & 1 \end{bmatrix} \quad \text{and} \quad \mathcal{H}'_i(z) = [\Psi^{-1}]_{i,*} \Gamma (zI - A)^{-1} B \quad (68)$$

and $[\Psi^{-1}]_{i,*}$ denotes the i th row of Ψ^{-1} .

10.1 Prediction horizon $N = 1$:

When the prediction horizon is $N = 1$, $\Psi = 1$ since $h_0 = 1$ and

$$\mathcal{H}(z) = 1 + \mathcal{H}'_1(z) = 1 + C(zI - A)^{-1}B = H(z)$$

and the moving horizon implementation is

$$y(k) = q_{\tilde{\mathbb{U}}^N} [H(z)w(k) - [H(z) - I]y^*(k)]. \quad (69)$$

and $q_{\tilde{\mathbb{U}}^N}[\cdot] = q_{\mathbb{U}}[\cdot]$ for $\Psi = 1$ and it becomes scalar (direct) quantisation.

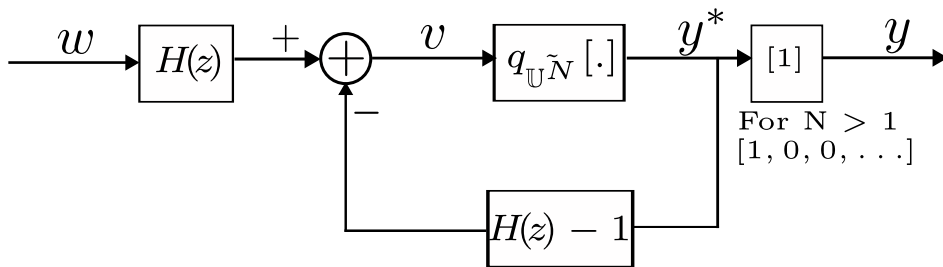


Figure 21: NSD equivalent of MHOQ implementation for $N = 1$.

10.2 Prediction horizon $N = 2$:

When the prediction horizon is $N = 1$, $\Psi = \begin{bmatrix} h_0 & 0 \\ h_1 & h_0 \end{bmatrix}$ and thus $\Psi^{-1} = \frac{1}{h_0^2} \begin{bmatrix} h_0 & -h_1 \\ 0 & h_0 \end{bmatrix} = \begin{bmatrix} 1 & -h_1 \\ 0 & 1 \end{bmatrix}$ since $h_0 = 1$. We get,

$$\begin{aligned}\mathcal{H}'_1(z) &= [1 \quad -h_1] \Gamma(zI - A)^{-1}B = (C - h_1CA)(zI - A)^{-1}B = H(z) - h_1CA(zI - A)^{-1}B - 1 \\ \mathcal{H}'_2(z) &= [0 \quad h_0] \Gamma(zI - A)^{-1}B = CA(zI - A)^{-1}B\end{aligned}$$

Then

$$\mathcal{H}(z) = \begin{bmatrix} 1 + \mathcal{H}'_1(z) & 0 \\ \mathcal{H}'_2(z) & 1 \end{bmatrix} = \begin{bmatrix} 1 + \mathcal{H}'_1(z) & 0 \\ \mathcal{H}'_2(z) & 1 \end{bmatrix} = \begin{bmatrix} H(z) - h_1CA(zI - A)^{-1}B & 0 \\ CA(zI - A)^{-1}B & 1 \end{bmatrix}$$

and the moving horizon implementation is

$$\begin{aligned}y(k) &= [1, 0] \Psi^{-1} q_{\tilde{U}^N} [\Psi \{ \mathcal{H}(z) \mathbf{w}(k) - [\mathcal{H}(z) - I] \mathbf{y}^*(k) \}] \\ &= [1, 0] \Psi^{-1} q_{\tilde{U}^N} [\Psi \mathcal{H}(z) \mathbf{w}(k) - \Psi [\mathcal{H}(z) - I] \mathbf{y}^*(k)] \\ &= [1, 0] \Psi^{-1} q_{\tilde{U}^N} [\Psi \mathcal{H}(z) (\mathbf{w}(k) - \mathbf{y}^*(k)) + \Psi \mathbf{y}^*(k)] \\ &= [1, 0] \Psi^{-1} q_{\tilde{U}^N} \left[\begin{bmatrix} H(z) - h_1CA(zI - A)^{-1}B & 0 \\ h_1H(z) - (h_1^2 - 1)CA(zI - A)^{-1}B & 1 \end{bmatrix} \mathbf{w}(k) - \begin{bmatrix} H(z) - 1 - h_1CA(zI - A)^{-1}B & 0 \\ h_1(H(z) - 1) - (h_1^2 - 1)CA(zI - A)^{-1}B & 0 \end{bmatrix} \mathbf{y}^*(k) \right] \\ &= [1, 0] \Psi^{-1} q_{\tilde{U}^N} \left[\begin{bmatrix} H(z) & 0 \\ 0 & 0 \end{bmatrix} \mathbf{w}(k) - \begin{bmatrix} H(z) - 1 & 0 \\ 0 & 0 \end{bmatrix} \mathbf{y}^*(k) \right. \\ &\quad \left. + \begin{bmatrix} -h_1CA(zI - A)^{-1}B & 0 \\ h_1H(z) - (h_1^2 - 1)CA(zI - A)^{-1}B & 1 \end{bmatrix} \mathbf{w}(k) - \begin{bmatrix} -h_1CA(zI - A)^{-1}B & 0 \\ h_1(H(z) - 1) - (h_1^2 - 1)CA(zI - A)^{-1}B & 0 \end{bmatrix} \mathbf{y}^*(k) \right]\end{aligned}$$

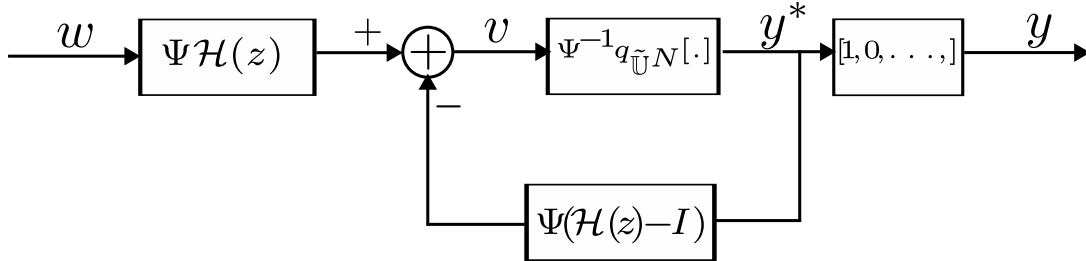


Figure 22: NSD equivalent of MHOQ implementation for $N > 2$.

References

- [1] Shuichi Ohno and M. Rizwan Tariq. Optimization of noise shaping filter for quantizer with error feedback. *IEEE Transactions on Circuits and Systems I: Regular Papers*, 64(4):918–930, 2017.
- [2] Izumi Masubuchi, Atsumi Ohara, and Nobuhide Suda. Lmi-based controller synthesis: A unified formulation and solution. *International Journal of Robust and Nonlinear Control*, 8(8):669–686, 1998.
- [3] Graham C Goodwin, Daniel E Quevedo, and David McGrath. Moving-horizon optimal quantizer for audio signals. *Journal of the Audio Engineering Society*, 51(3):138–149, 2003.

11 Scribble

We want to minimise this error: $\bar{e} = Hy - Hw = Hv + H\epsilon - Hw$

$$\bar{e} = Hy - Hw = Hv + H\epsilon - Hw$$

What is \bar{e} when

- the feedback filter is a (double) delay (standard delta-sigma)
- the feedback filter is optimal
- the feedback filter is implemented in the MPC formulation with horizon length 1, 2, 3, ...

Things to study

done Need to handle saturation (no need as optimal gain appears to be 3)

done What happens when there is a constant noise floor, unaffected by the noise-shaping (no need as small headroom is sufficient for gain of 3)

- Can we limit the rate
- Adding in INL

Total noise and distortion:

$$\sigma_t = \sigma_n + \sigma_q$$

$$\frac{\sigma_s}{\sigma_n + \sigma_q}$$